JOURNAL OF BACTERIOLOGY, July 1997, p. 4501–4512 Vol. 179, No. 14
0021-9193/97/$04.00+0

The *kdp* System of *Clostridium acetobutylicum*: Cloning, Sequencing, and Transcriptional Regulation in Response to Potassium Concentration

ANKE TREUNER-LANGE,[1,2] ANITA KUHN,[2] AND PETER DÜRRE[1,2]*

Angewandte Mikrobiologie und Mykologie, Universität Ulm, D-89069 Ulm,[1] and Institut für Mikrobiologie, Georg-August-Universität Göttingen, D-37077 Göttingen,[2] Germany

Received 30 September 1996/Accepted 14 April 1997

The complete sequence of the *kdp* gene region of *Clostridium acetobutylicum* has been determined. This part of the chromosome comprises two small open reading frames (*orfZ* and *orfY*), putatively encoding hydrophobic peptides, and the genes *kdpA*, *kdpB*, *kdpC*, and *kdpX*, followed by an operon encoding a pair of sensor-effector regulatory proteins (KdpD and KdpE). Except for *orfZ*, *orfY*, and *kdpX*, all genes showed significant homology to the *kdp* genes of *Escherichia coli*, encoding a high-affinity potassium transport ATPase and its regulators. The complete genome sequence of *Synechocystis* sp. strain PCC 6803 and a recently published part of the *Mycobacterium tuberculosis* genome indicate the existence of a *kdp* system in these organisms as well, but all three systems comprise neither a second *orf* upstream of *kdpA* nor an additional *kdpX* gene. Expression of the clostridial *kdp* genes, including the unique *kdpX* gene, was found to be inducible by low potassium concentrations. A transcription start point could be mapped upstream of *orfZ*. A promoter upstream of *kdpD* was active only under noninducing conditions. Lowering the potassium content of the medium led to formation of a common transcript (*orfZYkdpABCXDE*), with a putative internal RNase E recognition site, which could be responsible for the instability of the common transcript. Except for the two small peptides, all gene products could be detected in in vitro transcription-translation experiments.

Regulation of the potassium content of the cytoplasm is the primary response of bacterial cells to osmotic stress (11, 23). A number of different K^+ transporters are known; these include uptake systems such as TrkG, TrkH, Kup, and Kdp (in *Escherichia coli*) as well as efflux systems such as the enterobacterial KefB, KefC, antiporters, colicin, and stretch-activated channels (for reviews, see references 7, 8, and 49).

Of these, Kdp of *E. coli* is the best-studied bacterial K^+ uptake system (for reviews, see references 2 and 46). It is an atypical P-type ATPase, consisting of three cytoplasmic membrane proteins, KdpA, KdpB, and KdpC, and probably a small hydrophobic peptide (KdpF). The transporter is induced by potassium limitation and changes in medium osmolarity. It is a high-affinity system that uses ATP as the driving force for K^+ uptake. The genes encoding the four different subunits are organized in a common operon, whose expression is controlled by a sensor kinase and response regulator (KdpD and KdpE). The respective genes, *kdpD* and *kdpE*, are organized in an operon directly downstream of *kdpFABC* (40, 57). However, little is known about *kdp*-analogous systems from other bacteria. DNA-DNA hybridization experiments indicated its presence in other enterobacteria, cyanobacteria, *Pseudomonas aeruginosa*, and *Spiroplasma citri* (47, 56). The solubilization of Kdp-ATPase complexes is described for *E. coli* (45), for *Alicyclobacillus acidocaldarius* (formerly *Bacillus acidocaldarius* [29]), and *Rhodobacter sphaeroides* (1), both including immunological cross-reactivity of KdpB with antibodies against the enterobacterial ATPase, and there is no evidence for a fourth subunit within the complexes.

Recently, genes of a two-component regulator system from the gram-positive, obligately anaerobic spore former *Clostridium acetobutylicum* have been cloned and sequenced. They showed significant homology to *kdpD* and *kdpE* of *E. coli* (52). This report describes sequencing and analysis of the adjacent DNA region, which was found to comprise a *kdp*-homologous system with, however, several significant differences from the enterobacterial complex and from the sequences of *Mycobacterium tuberculosis* (*Mycobacterium tuberculosis* sequencing project [http://www.sanger.ac.uk/pathogens/]) and *Synechocystis* sp. strain PCC 6803 (30).

MATERIALS AND METHODS

Bacterial strains, plasmids, and growth conditions. *C. acetobutylicum* DSM 792 was used as a source of genomic DNA and total RNA. The organism was grown under strictly anaerobic conditions at 37°C in clostridial basal medium (38) or in a minimal medium which contained, per liter, the following: glucose, 40 g; 2-[*N*-morpholino]ethanesulfonic acid (MES), 21.3 g; NaH_2PO_4, 1.4 g; $(NH_4)_2SO_4$, 2 g; $MgSO_4$, 0.1 g; NaCl, 10 mg; $Na_2MoO_4 \cdot 2H_2O$, 10 mg; $CaCl_2 \cdot 2H_2O$, 10 mg; $MnSO_4 \cdot H_2O$, 15 mg; $FeSO_4 \cdot 7H_2O$, 15 mg; *p*-aminobenzoic acid, 2 mg; thiamine hydrochloride, 2 mg; biotin, 0.1 mg; and $Na_2S_2O_4$, 35 mg. The fermentation medium for the potassium-limited chemostat experiments was the same as above except that no MES was added and a pH of 2 was adjusted with H_2SO_4. The chemostat experiments were performed in a fermentor with 1,000-ml culture volume, the temperature was held at 37°C by an external water bath, the pH was measured with a glass electrode (Dr. W. Ingold KG, Frankfurt, Germany), maintained at the desired value (6.0) by automatic addition of 2 N NH_3, and the culture volume was maintained constant by providing an overflow pipe for gases and cell suspension. In the first limitation experiment, the starting potassium concentration was approximately 6 mM, using KCl as the potassium source. By addition of minimal medium without potassium at a dilution rate of 50 ml/h, the potassium concentration was slowly decreased to 50 μM within 100 h. The second limitation experiment started at a concentration of 1.5 mM KCl, which was decreased to 0.13 mM potassium at a dilution rate of 150 ml/h within 16 h.

E. coli JM109 (58), *E. coli* JM83 (58), and *E. coli* SURE (Stratagene GmbH, Heidelberg, Germany) were used as hosts, and pUC9 (53) and pEcoR252 (kindly supplied by D. R. Woods, University of Cape Town, Cape Town, South Africa) were used as vectors for cloning experiments and genomic library constructions. *E. coli* was grown aerobically in Luria broth or on Luria agar (41), supplemented with ampicillin (100 μg/ml) when required for plasmid selection and maintenance.

* Corresponding author. Mailing address: Angewandte Mikrobiologie und Mykologie, Universität Ulm, D-89069 Ulm, Germany. Phone: 49-731-502-2710. Fax: 49-731-502-2719. E-mail: peter.duerre@biologie.uni-ulm.de.

Measurement of potassium concentration. Cells from 1 ml of culture were separated by centrifugation, and the potassium concentration of the supernatant was determined by flame photometry.

Measurement of optical density. The optical density at 600 nm (OD_{600}) was measured in a spectrophotometer (Spectronic 601; Milton Roy, Ostende, Belgium). The light path was 1 cm.

Nucleic acid isolation and manipulation. Chromosomal DNA of *C. acetobutylicum* was isolated by the method of Marmur (35), with the modifications described by Bertram and Dürre (10). For isolation of plasmids from *E. coli*, a Qiagen Midi kit (Qiagen GmbH, Hilden, Germany) was used. Total RNA of *C. acetobutylicum* was isolated with the hot phenol-chloroform procedure of Oelmüller et al. (39) as modified by Gerischer and Dürre (28). DNA and RNA were manipulated by standard methods (41); restriction endonucleases and other modifying enzymes used were obtained from a variety of sources and used according to the manufacturers' instructions.

PCR. PCR amplifications were performed in 100-μl volumes containing primers (0.5 μM each) and chromosomal DNA (50 to 500 ng). When *Taq* polymerase (AGS GmbH, Heidelberg, Germany) was used, reactions were performed with 2 U of polymerase in 20 mM Tris hydrochloride (pH 8.55)–16 mM $(NH_4)_2SO_4$–1.5 mM $MgCl_2$–deoxynucleoside triphosphates (dNTPs; 50 μM each) covered with paraffin oil. For amplifications of fragments that were to be used for further cloning procedures, 2 to 4 U of Vent polymerase was used in 10 mM KCl–10 mM $(NH_4)_2SO_4$–20 mM Tris hydrochloride (pH 8.8)–2 to 6 mM $MgSO_4$–0.1% Triton X-100 covered with paraffin oil. Temperature cycling was performed by a programmable thermocycler (Trio-Thermoblock; Biometra biomedizinische Analytik GmbH, Göttingen, Germany) with the following conditions: 95°C for 5 min (without enzyme), cooling to 80°C, and addition of enzyme, 95°C for 30 s, $T_{d\,(\text{primer 1 or 2})}$ − 5°C (50) for 30 s, and 72°C for 1 min/1,000 bp for 35 cycles.

Primers. Synthetic oligodeoxynucleotides as primers for sequencing and PCR were prepared with a Gene Assembler Plus (Pharmacia Biotech Europe GmbH, Freiburg, Germany) as instructed by the manufacturer. The following primers (in 5′-to-3′ direction; numbers indicate the position of each primer within the *kdp* region) for PCR amplification, dot blot hybridization, and reverse transcriptase PCR (RT-PCR) were used: for RT-PCR, CTTTTAATGTGTAATGC (*kdpA*$_9$, 1106 to 1122), CTATTTGCTAATTTTGC (*kdpA*$_{20}$, 2834 to 2850), TAAGTGC ATCTGCTTGA (*kdpA*$_{21}$, 2897 to 2881), TAGCAATACCAAAAATG (*kdp*9.1, 4386 to 4402), TCCACCAAAACCAAATAC (*kdpB*$_2$, 4579 to 4562), GAAAA TTCACTTTTGTA (*kdp*9.9, 5299 to 5315), GGATTGATAATAAATAT (*kdp*9.10, 5539 to 5555), TAGATAAGGAAGAAAAA (*kdp*9.11, 5755 to 5771), GATGTGTACACCACTTT (*kdp*9.13, 6126 to 6142), GTCTGTAAATCTCT TTA (*kdpD*$_6$, 6296 to 6280), ATTATTCTTGCCGAAGA (*kdpD*$_7$, 6517 to 6501), ATGGATGATATTATCCC (*kdp*9.22, 7081 to 7065), TACATTCCTATAAA AAT (*kdpD*$_5$, 7545 to 7562), CATCTATAAGTTCTCCA (*kdp*9.15, 7836 to 7820), TCGCTATATTTATAGCC (*kdp*9.5, 8519 to 8503), and TTTTATACTC TATTGGC (*kdp*9.2, 8914 to 8898); for the *kdpCXD* probe, CTAGCTCGGGC TCTGGA (*kdp*9.8, 5066 to 5082) and *kdpD*$_6$; for the *kdpA* probe, *kdpA*$_9$ and TTTATTTCTTTGCCTTC (*kdpA*$_{22}$, 2145 to 2129); for the *kdpX* probe, *kdp*9.9 and CCCTTGAAAATGCCTT (*kdpD*$_2$, 5597 to 5581); for the *kdpDE* probe, GGGGTACCGAACTAAAATCAGTT (*kdpE*$_6$, 9161 to 9145) and CTTTTAG ATAATGCTTC (*kdpE*$_4$, 8103 to 8119); for cloning of pTC, CGGGATCCCGT TAATTTAGGATAGA (*kdpC*$_{Bam\text{HI linker}}$, 4644 to 4658) and CCGCTCGAGC TGAATTTCTCATTA (*kdpC*$_{Xho\text{I linker}}$, 5307 to 5293); and for quantitative dot blot hybridizations, ACACCCGCTGCATAGCC (*kdpD*$_3$, 5821 to 5805), *kdpD*$_2$, and TGCCCTACTGCCGTTAT (*kdpC*$_{12}$, 4769 to 4753).

Genomic libraries of *C. acetobutylicum*. Chromosomal DNA of strain DSM 792 was partially digested with *Sau*3AI and ligated in *Bam*HI-digested pUC9 (27) or in *Bgl*II-digested pEcoR252 (25). A third library used resulted from digestion of chromosomal DNA of strain DSM 792 with *Hin*dIII, fractionation by sucrose density centrifugation, and ligation of the fraction containing fragments of 0.8 to 3.5 kbp into *Hin*dIII-digested pUC9 (42). Colony hybridization using Hybond N nylon filters (Amersham Buchler GmbH, Braunschweig, Germany) was used for screening the genomic libraries. The colony filters were prepared as described by Buluwela et al. (13).

Nucleic acid hybridizations. For dot blots, 10 μg of RNA was incubated at 65°C for 5 min in 3 volumes of a solution consisting of 500 μl of formamide, 162 μl of formaldehyde (37%, vol/vol), and 100 μl of 10× MOPS buffer (0.2 M 3-[*N*-morpholino]propanesulfonic acid, 0.5 M sodium acetate [pH 7.0], 0.01 M Na_2EDTA). After addition of 1 volume of cold 20× SSC (3.0 M NaCl, 0.3 M sodium citrate; 1× SSC is 0.15 M NaCl plus 0.015 M sodium citrate) the RNA samples were spotted onto a Hybond N nylon membrane (Amersham Buchler), prewetted in 10× SSC. RNA was fixed onto the membranes by UV cross-linking (direct contact of the RNA-containing side for 2 min at 254 nm on a Croma 41 UV transilluminator [Vetter, Germany] or for 5 min at 312 nm on a dual light transilluminator [MWG-Biotech GmbH, Ebersberg, Germany]). For Northern blots, 10 μg of RNA was separated in 0.8% (wt/vol) denaturing formaldehyde agarose gels and transferred to Hybond N nylon membranes (Amersham Buchler).

For hybridization with DNA fragments of >100 bp, membranes were prehybridized in 0.2% (wt/vol) polyvinylpyrrolidone–0.2% (wt/vol) Ficoll 400–0.2% (wt/vol) bovine serum albumin–50 mM Tris hydrochloride (pH 7.5)–0.1% (wt/vol) sodium pyrophosphate–10% (wt/vol) dextran sulfate–1% (wt/vol) sodium dodecyl sulfate (SDS)–1 M NaCl for 0.5 to 2 h at 55°C. The DNA fragments were radiolabeled with [α-^{32}P]dATP (Hartmann Analytic GmbH, Braunschweig, Germany) by using a random primers labeling kit (GIBCO/BRL GmbH, Eggenstein, Germany). The labeled probes were purified by using Sephadex G-25 columns (NAP-5; Pharmacia Biotech Europe). For hybridization with oligonucleotides, membranes were prehybridized in 0.15% (wt/vol) polyvinylpyrrolidone–0.15% (wt/vol) Ficoll 400–0.15% (wt/vol) bovine serum albumin–90 mM Tris hydrochloride (pH 7.5)–6 mM Na_2EDTA–1% (wt/vol) SDS–salmon sperm DNA (1 mg/ml)–1 M NaCl for 0.5 to 2 h at T_d − 5°C (50). The oligonucleotides (17 pmol, 17-mer) were radiolabeled with 50 μCi of [γ-^{32}P]dATP (Amersham Buchler) and purified with a QIAquick nucleotide removal kit (Qiagen). After addition of radiolabeled probes to the prehybridization solution, hybridization was continued for 10 to 12 h. Membranes were then washed in 2× SSC (DNA probes of >100 bp, 45°C) or 6× SSC (oligonucleotides, T_d − 10°C) and subjected to autoradiography.

Quantification of hybridization results. For quantification of hybridization signals, the membranes were subjected to autoradiography using Fujifilm BAS Phosphor Images plates (Fuji Photo Film Europe GmbH, Düsseldorf, Germany). The image plates were scanned with a BAS 1000 Image Reader (Fuji Photo Film Europe), and the scanned images were analyzed in the quantifications mode of the Mac Bas version 2.3 software (Fuji Photo Film Europe). Another method used was autoradiography with conventional X-ray films, scanning the films with a Umax Power Look scanner using the corresponding plug-in image-scanning MagicScan program that runs under Photoshop on a Macintosh computer (UMAX Data Systems Inc., Taipei, Taiwan). The TIFF-formatted images were analyzed with the Intelligent Quantifier software (Bio Image U.K., Cheshire, England). Pict-formatted images were analyzed with the Mac Bas Version 2.3 program (Fuji Photo Film Europe).

DNA sequencing and sequence analysis. The nucleotide sequence of the double-stranded plasmid DNA was determined by primer walking according to the dideoxy-chain termination method, using a T7 sequencing kit (Pharmacia Biotech Europe). All nucleotide data presented were confirmed by sequencing both strands of the inserts. The dideoxy-terminated fragments were separated on 55-cm wedge-shaped thickness gradient gels (0.2 to 0.4 mm, 6% [wt/vol] polyacrylamide) with a Macrophor sequencing unit (Pharmacia Biotech Europe) as recommended by the manufacturer. The obtained sequence data were analyzed by using the DNA Strider (34) and GeneWorks (IntelliGenetics, Inc., Mountain View, Calif.) programs. Sequence comparison results and CodonPreference results were obtained with the Bestfit program of the Genetics Computer Group sequence analysis software package (Wisconsin Package version 9.0; Genetics Computer Group, Madison, Wis.) (20).

Nonradioactive determination of the transcription start point. The IRD41-labeled oligonucleotides *kdpA*$_p$ (GTACGAACACAATAAGAATA [950 to 931]) and *orfZ*$_p$ (AAAAGCCTAGAACTATTAAT [738 to 719]) were obtained from MWG-Biotech and were used to determine a transcription start point upstream of *kdpA*. The annealing of 0.2 pmol of each primer was performed in a total volume of 10 μl containing 10 μg of total RNA, 10 mM Tris hydrochloride (pH 7.9), 0.5 M KCl, and 12.5 U of human placenta RNase inhibitor (GIBCO/BRL). After heating for 5 min at 80°C, the annealing reactions were incubated for 3 h at 30°C. For a 50-μl primer extension reaction, 10 μl of 5× reverse transcription buffer (250 mM Tris hydrochloride [pH 8.3], 125 mM KCl, 50 mM dithiothreitol, 15 mM $MgCl_2$), 500 μM dNTPs, 2.5 μg of actinomycin D, 200 U of SuperScript II (GIBCO/BRL), and H_2O were added to the annealing reaction mixtures and incubated for 1 h at 37°C. The primer extension products were phenol-chloroform extracted, ethanol precipitated, and analyzed on a 6% polyacrylamide sequencing gel running on a LI-COR model 4000L DNA sequencer (MWG-Biotech) as instructed by the manufacturer. The length of each of the primer extension reaction products was determined by running sequence reactions with the same primers on the same gel. The sequencing reactions were performed with the SequiTherm cycle sequencing kit for LI-COR (Biozym Diagnostik GmbH, Hessisch Oldendorf, Germany), using a MultiCycler PTC 200 (Biozym Diagnostik).

RT-PCR. cDNA synthesis was performed by reverse transcription of RNA primed with different sequence-specific oligonucleotides. The reverse transcriptase used was SuperScript II, obtained from GIBCO/BRL. After priming of the oligonucleotide (1 to 20 pmol) in 0.5 M KCl–10 mM Tris hydrochloride (pH 7.9), in the presence of 12.5 U of human placenta RNase inhibitor and 5 to 10 μg of RNA, for 3 h at 30°C, the reaction mixture was divided into two parts. The first aliquot was brought to a final concentration of 50 mM Tris hydrochloride (pH 8.3)–25 mM KCl–3 mM $MgCl_2$–10 mM dithioerythritol–0.5 mM dNTPs–0.5 mg of actinomycin D. The second aliquot was treated the same way but received additionally 200 U of reverse transcriptase. Both mixtures were incubated for 1 h at 37°C and were used directly as templates in the following PCRs. As a further control, additional reactions were performed with plasmid or chromosomal DNA as a template, using the same master mix containing all necessary components for all assays.

In vitro transcriptions and translations. ^{35}S-labeled proteins were synthesized by using an *E. coli* S30 extract system for circular DNA (Promega Corp., Madison, Wis.) with ^{35}S-labeled methionine (Hartmann Analytic). After an acetone precipitation, the labeled translation products were analyzed on SDS–4 to 20% and 12 to 20% (wt/vol) polyacrylamide gradient gels and visualized by autoradiography. Protein size was determined by using ^{14}C-methylated protein molecular weight markers in a range of 14,300 to 200,000 (Amersham Buchler) and the

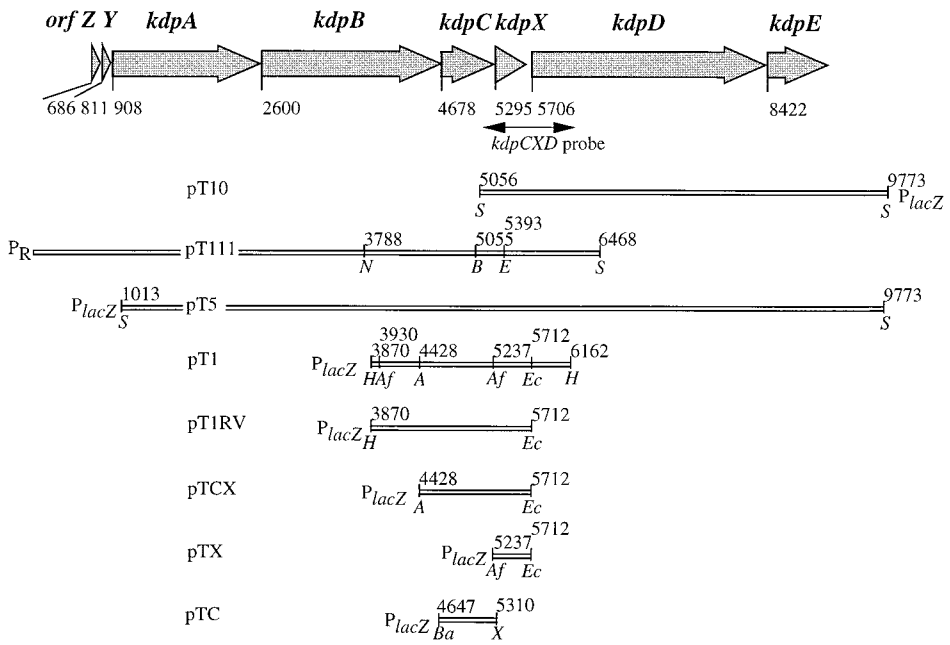

FIG. 1. Schematic representation of the *kdp* genes from *C. acetobutylicum*. The positions of the ATG start codons of the *kdp* genes (grey arrows) are indicated by numbers. The line with arrowheads at both ends indicates the *kdpCXD* probe used for screening of the different gene libraries of *C. acetobutylicum*. The 4,718-bp insert of pT10 (52) is shown, as well as the insert positions of the new positive clones pT111, pT5, and pT1. Clones pT1RV, pTCX, and pTX were constructed by different deletions from pT1. pTC is the product of cloning a PCR fragment with a *Bam*HI and an *Xho*I linker. Positions of the promoters of pUC9 (P_{lacZ}) and of pEcoR252 (P_R) are indicated. Numbers and letters represent restriction sites and their positions within the *kdp* gene region. Abbreviations: A, *Acc*I; *Af*, *Afl*II; *Ba*, *Bam*HI; *B*, *Bgl*II; *E*, *Eco*NI; *Ec*, *Eco*RV; *H*, *Hin*dIII; *N*, *Nde*I; *S*, *Sau*3AI; *X*, *Xho*I.

positive control reaction of the kit, showing the 60.7-kDa luciferase, a 48-kDa band due to an internal start site in the luciferase sequence, and the 31.5-kDa β-lactamase.

Nucleotide sequence acession number. The sequence data shown in Fig. 2 were submitted to the EMBL database and assigned accession no. U44892.

RESULTS

Cloning and sequencing of the complete *kdp* DNA. For cloning of the upstream region of *kdpDE* (52), a DNA probe was generated by PCR using a primer pair (*kdp*9.8-*kdpD*$_6$) from the 5′ end of the available *kdpDE* inserts. This 1,214-bp probe was used for screening of three different genomic libraries of *C. acetobutylicum*. Hybridization experiments allowed us to identify three new clones (pT1, pT5, and pT11) in addition to the already sequenced clone pT10 (52). pT1 contained a 2,298-bp *Hin*dIII fragment in the vector pUC9 (Fig. 1). The 8,368-bp pT5 insert consisted of a partially *Sau*3AI-digested fragment in the vector pUC9. Sequence analysis of the 5′ and 3′ ends of pT5 showed that the pT5 sequence contained two open reading frames (ORFs) in addition to the genes *kdpC*, *kdpX*, *kdpD*, and *kdpE* (52). The first ORF was truncated; the deduced amino acid sequence showed significant homology to the KdpA protein of *E. coli* and was named accordingly. The second ORF was identified as the *kdpB*-homologous gene of *C. acetobutylicum* and was thus designated *kdpB*. To determine the missing part of *kdpA* and the promoter region, the pT11 clone was sequenced by primer walking. The 7,940-bp pT11 insert represented a *Sau3*AI fragment ligated in the vector pEcoR252. The 3′ end of the insert was located within the *kdpD* gene and contained approximately 2,400 additional bp upstream of the *kdpA* ATG start codon. For sequence analysis, a subclone (pT111) was constructed by deletion of a 1,562-bp *Sty*I fragment, creating blunt ends, and ligation into pEcoR252. The resulting plasmid, pT111, contained a 6,474-bp insert (Fig. 1). The nucleotide sequence of the *kdp* region was determined, and the heretofore unpublished sequence (starting with the *Sty*I restriction site of pT111 and including the complete *kdpC* gene) is presented in Fig. 2. The *kdp* region of *C. acetobutylicum* consists of eight ORFs (Fig. 1), all of which start with ATG start codons that are preceded by putative ribosome-binding sites (Fig. 2) (52). The designations of the ORFs and their positions within the *kdp* region, lengths, and G+C contents are summarized in Table 1. The DNA sequences of *orfZ*, *orfY*, and *kdpX* had a significantly lower G+C content than the genes *kdpA*, *kdpB*, *kdpC*, *kdpD*, and *kdpE*.

Amino acid similarities and features of the deduced Kdp proteins from *C. acetobutylicum*. The deduced amino acid sequences encoded by the *C. acetobutylicum kdpA*, *kdpB*, *kdpC*, and *kdpX* genes were used to search the different nucleic acid and protein databases with the BLAST computer program (3). As expected, there was considerable sequence similarity between the different KdpA proteins (Table 2) and the clostridial KdpA, consisting of 556 amino acids with a deduced M_r of 60,077. The KdpA protein of *E. coli* is predicted to span the membrane with 12 α helices based on the hydrophobicity of the protein (22) or with at least 10 α helices (14). Hydrophobicity plots (31) of the clostridial KdpA and the enterobacterial KdpA showed almost identical patterns, including hydrophobic regions long enough to be membrane-spanning segments (data not shown). Nine amino acid residues, suggested to form a periplasmic K^+-binding site in the *E. coli* KdpA (14), are conserved in the clostridial KdpA. However, of the four residues assumed to be part of the cytoplasmic K^+-binding site in *E. coli* (14), only two are conserved in the protein of *C. acetobutylicum.*

The 2,055-bp *kdpB* gene encodes a protein with 685 amino acids yielding a calculated M_r of 73,751. KdpB of *C. acetobutylicum* showed significant homology to a number of other

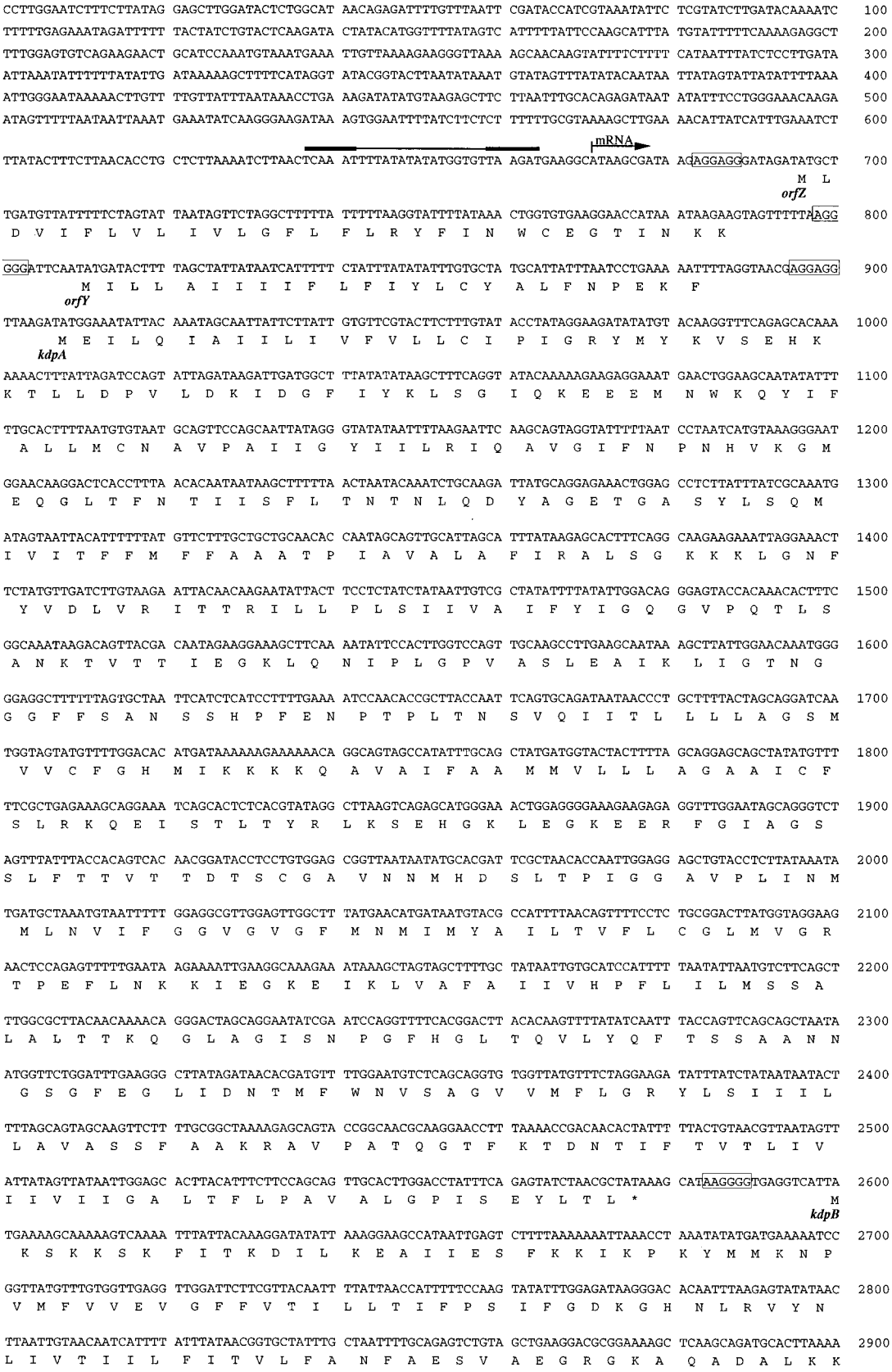

FIG. 2. Nucleotide sequence of *orfZ*, *orfY*, *kdpA*, *kdpB*, and *kdpC* of *C. acetobutylicum*. The deduced amino acid sequences are provided in single-letter code below the DNA sequence. Putative ribosome-binding sites are boxed. The putative promoter region is marked by thick solid bars above the −10 and −35 regions joined by a line. The determined mRNA start point is marked by an arrow. Translation stop signals are marked by asterisks below the codon.

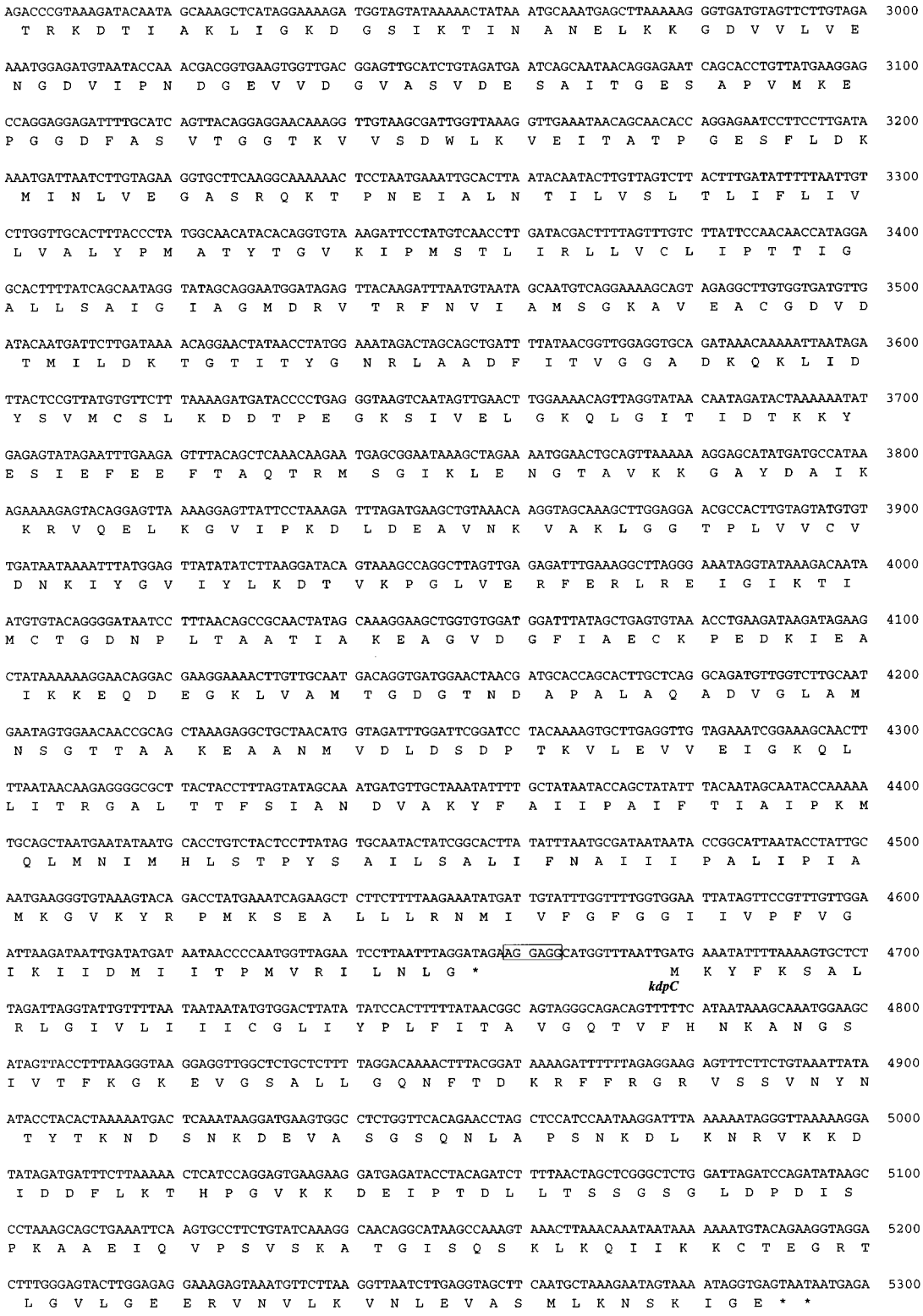

FIG. 2—*Continued.*

TABLE 1. Features of the different ORFs of the *kdp* system of *C. acetobutylicum*

ORF	Position (nucleotides)	Length (bp)	G+C content (mol%)
orfZ	696–789	93	26
orfY	811–886	75	19
kdpA	908–2576	1,668	35
kdpB	2600–4655	2,055	35
kdpC	4678–5290	612	33
kdpX	5295–5637	342	24
kdpD	5706–8406	2,700	33
kdpE	8422–9118	696	35

proteins. The highest value could be determined for the KdpB proteins of *Synechocystis* sp. strain PCC 6803, *M. tuberculosis*, and *E. coli* (Table 2). The next matches with decreasing homology are all characterized as P-type ATPases or E_1-E_2 ATPases (Table 2). The highest similarities within the different P-type ATPases were found within cluster 4 described by Fagan and Saier (24), including all bacterial P-type ATPases except a Mg^{2+}-ATPase of *S. typhimurium* (48). The three most conserved regions of P-type ATPases (24) could be identified in the clostridial KdpB. The motif (DNS)(QENR)(SA)(LIVAN)(LIV)(TSN)**GE**(SN) (24) is conserved in the clostridial KdpB with the amino acid sequences DESAIT**GE**S. Like KdpB of *E. coli* (32), the clostridial KdpB has a short C-terminal region and only one pair of possible transmembrane segments before the TGES sequence. The motif (LIV)(CAML)(STFL)**DKTGT**(LI)T, which is the essential phosphorylation site, was represented by the clostridial sequence MIL**DKTGT**IT. The last very well conserved motif, (TIV)**GDG**X**ND**(ASG)**P**(ASV)**L**, belongs to the ATP-binding site (24), and in *C. acetobutylicum*, the corresponding sequence T**GDGTNDAPAL** could be found.

The *kdpC* gene was found to consist of 612 bp and encodes a protein of 204 amino acids with a calculated M_r of 22,187. KdpC of *C. acetobutylicum* showed similarities with the other KdpC proteins as expected (Table 2). Hydropathy analysis of the KdpC proteins led to predicting strongly hydrophobic N-terminal transmembrane segments (data not shown).

The *kdpX* gene would encode a protein of 114 amino acids with a calculated M_r of 13,465. KdpX did not show significant homology to other known protein sequences, but it resembles some prokaryotic and eukaryotic proteins shown in Table 2, including KdpC of *E. coli* in an N-terminal hydrophobic region. Nothing is known about the function of the predicted *orf27* product from *Helicobacter pylori*. In a distance of ca. 4,000 bp, another ORF (*orf32*), encoding a protein which resembles the potassium efflux system protein KefC of *E. coli*, has been detected. However, any possible functional relationship would be purely speculative without further experimental evidence. The three ATPase synthase proteins 8 of the different *Drosophila* spp. (Table 2) are all described as a membrane-bound nonenzymatic component of the mitochondrial ATPase complex. Within the first N-terminal amino acids, there are several conserved residues in KdpC of *E. coli* and in KdpC of *C. acetobutylicum* as well as in the clostridial KdpX (Fig. 3). KdpC in the Kdp-ATPase of *E. coli* seems to play a role in assembly of the complex or the subunits KdpA and KdpB, because KdpA/B aggregates are not formed without KdpC (49).

The two ORFs upstream of *kdpA* seem to have peptide-coding function because of the translational signals (Fig. 2). The first ORF, as designated *orfZ*, consists of 93 bp and would encode a small, rather hydrophobic peptide with 31 amino acids. The second ORF was designated *orfY*. The 75-bp *orfY* would also encode a small, rather hydrophobic peptide. The KdpF peptide of *E. coli* is likewise encoded by an ORF of 29 codons just upstream of *kdpA* (46). Upstream of *kdpA* of *M. tuberculosis*, we found another small ORF, encoding likewise a small hydrophobic peptide with 32 amino acids. In Table 2, this ORF is designated KdpF, in analogy to the Kdp system of *E. coli*. In the genome sequence of *Synechocystis* sp. strain PCC 6803, we could find no similarly small ORF.

In vitro transcription-translation experiments. Proteins of the sizes expected for KdpB, KdpD, and KdpE were produced in a coupled in vitro transcription-translation assay of clones pT11 and pT5 (Fig. 4). In case of the 60,077-Da clostridial KdpA, a protein band with an apparent M_r of approximately 50,000 was detectable, resembling the situation in *E. coli*, where the 59-kDa KdpA runs as a diffuse band with an apparent M_r of 49,000 in an SDS-gel (45). No distinct protein that might represent the proteins KdpC and the putative KdpX could be detected. In a second in vitro transcription-translation experiment, the constructed subclones pTC, pTCX, and pTX

TABLE 2. Amino acid similarity of the Kdp peptides and proteins from *C. acetobutylicum* to corresponding proteins of other organisms

Organism	Protein (aa)	% Identity	% Similarity	Accession no.
OrfZ (31 aa)				
E. coli	KdpF (29)	45.5[a]	72.3[a]	P36937
M. tuberculosis	OrfY (32)	45.0[b]	60.0[b]	Z92539
OrfY (25 aa)				
M. tuberculosis	KdpF[c] *(32)*	45.0	60.0	Z92359
E. coli	KdpF (29)	41.7	70.8	P36937
KdpA (555 aa)				
Synechocystis sp.	KdpA (559)	55.1	45.3	D90910
E. coli	KdpA (557)	43.8	56.2	P03959
M. tuberculosis	KdpA (571)	41.8	51.8	Z92539
KdpB (685 aa)				
Synechocystis sp.	KdpB (691)	61.9	71.7	D90910
M. tuberculosis	KdpB (708)	55.9	68.8	Z92539
E. coli	KdpB (682)	55.4	67.5	P03960
M. tuberculosis	P-type ATPase (770)	32.0	41.6	1524193
Proteus mirabilis	P-type ATPase (829)	31.1	40.7	1353678
Synechococcus sp.	P-type ATPase (747)	29.5	41.8	584792
KdpC (204 aa)				
Synechocystis sp.	KdpC (191)	44.8	53.6	D90910
M. tuberculosis	KdpC (189)	40.1	50.3	Z92539
E. coli	KdpC (190)	37.7	48.6	P03961
KdpX (114 aa)				
Helicobacter pylori	Orf 27 (255)	31.0[d]	55.2[d]	1800178
Drosophila yakuba	ATP synthase protein 8 (53)	50.0[e]	60.7[e]	114481
D. melanogaster	ATP synthase protein 8 (53)	46.4[e]	60.7[e]	114480
D. simulans	ATP synthase protein 8 (53)	46.4[e]	60.7[e]	1703632
E. coli	KdpC (191)	23.7[f]	39.5[f]	P03961

[a] Result of an alignment over a length of only 11 amino acids (aa).
[b] Result of an alignment over a length of only 12 amino acids.
[c] This name was chosen in analogy to the Kdp system of *E. coli*, missing also the second Orf of the Kdp system of *C. acetobutylicum.*
[d] Result of an alignment over a length of only 29 amino acids.
[e] Result of an alignment over a length of only 28 amino acids.
[f] Result of an alignment over a length of only 38 amino acids.

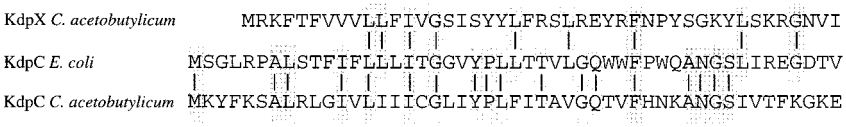

FIG. 3. Amino acid alignment of the proteins KdpC of *E. coli* and *C. acetobutylicum* and the clostridial KdpX. Amino acids identical among the sequences are boxed.

as well as pT1 (Fig. 1) and the vector control were used. Because of the small expected M_r of 22,187 (KdpC) and 13,465 (KdpX), we used an SDS–12 to 20% gradient gel for the separation (Fig. 5). We detected two bands which were not produced in the vector control. The putative KdpC showed some deviation from the expected mobility; the protein band corresponded to a molecular mass of ca. 27 kDa (Fig. 5).

K^+ limitation experiments and mRNA analysis. With total RNA from *C. acetobutylicum* cells growing in clostridial basal medium with ca. 38 mM potassium and harvested in the exponential acidogenic growth phase and the stationary solventogenic growth phase, it was not possible to determine a 5′ end of an mRNA upstream of *orfZ*, *orfY*, or *kdpA*, and there were no detectable Northern signals by hybridization experiments with different *kdp* probes. Since the genes *kdpA*, *kdpB*, and *kdpC* of *E. coli* encode an inducible high-affinity K^+-ATPase, which is induced only under K^+-limiting conditions, it seemed necessary to find conditions in which the clostridial *kdp* genes were induced. In two different chemostat experiments, the K^+ concentration was continuously decreased and RNA samples were taken at different stages of the limitation. K^+ concentration was determined in the cell-free supernatant of all samples. In the first limitation experiment, the starting potassium concentration was 6.04 mM K^+ (Fig. 6). Down to a potassium concentration of 600 μM, the optical density and thereby the population in the chemostat was not influenced by the limitation and consistently yielded values of 2.3. However, continued decreasing of the potassium concentration led to reduced optical density, and the growth of the population could no longer balance the dilution. A subsequent increase of K^+ to 5.24 mM restored the original OD_{600} of 2.3. Dot blot hybridization with a *kdpA* probe revealed that induction of the clostridial *kdpA* gene occurred when the potassium concentration was decreased. Highest induction occurred at potassium concentrations below 200 μM. Increasing the amount of K^+ again led to disappearance of the hybridization signals (Fig. 6). Growth impairment by the limitation paralleled the appearance of *kdpA* mRNA transcripts. Hybridization with *kdpB* and *kdpC* probes showed an identical pattern (data not shown). In a second limitation experiment, the potassium concentration was decreased from 1.5 mM to 130 μM (Fig. 7). Despite some fluctuations of the potassium concentration in this chemostat, it is evident that the optical density of the culture started to decrease at 0.49 mM K^+. *kdpA* and *kdpX* were clearly induced, but the hybridization signals with the *kdpX* probe yielded weaker signals although the same amount of RNA was used.

Using RNA samples 7 (first limitation; Fig. 6) and 4 (second limitation; Fig. 7), we determined the site of transcription initiation upstream of *kdpA* with two different primers. Primer extension reactions revealed in all cases a 5′ end of the mRNA 236 bp upstream of the *kdpA* start codon. The primer extension signals revealed with the $orfZ_p$ primer are shown in Fig. 8. This mRNA start point was preceded by a possible promoter sequence. The putative promoter (5′-TCAAT-16 bp-TAA GAT-3′ [Fig. 2]) showed only little homology to the consensus promoter of clostridia (5′-**T**TG**A**C**A**-17 bp-**TA**T**AAT-3′** [59]). The determined transcription start point of the *kdp* genes would allow transcription of the two small ORFs upstream of *kdpA*. The same RNA samples were used to confirm the mRNA start point upstream of *kdpD* (52) by primer extension ($kdpD_2$ served as a primer for the primer extension and sequencing reaction). No distinct signal of the expected size of 128 bp could be detected with these RNA samples, but there were a number of signals with larger and smaller sizes in the gel (data not shown). The same result was obtained when the adjacent oligonucleotide $kdpD_2$ was used.

RNA samples of the first limitation experiment were used for two identically prepared Northern blots. The first blot was hybridized with a *kdpA* probe (1,039 bp); the second was hybridized with a *kdpDE* probe (1,058 bp, last 300 bp of the *kdpD*

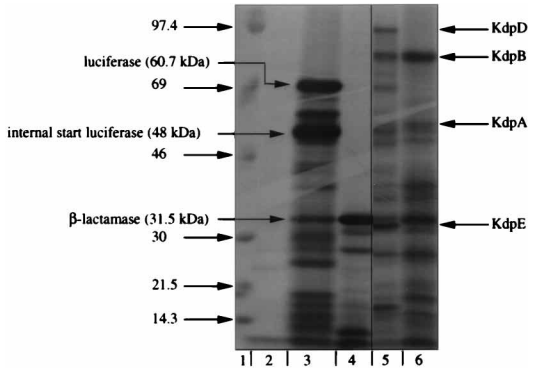

FIG. 4. Protein analysis of in vitro transcription-translation reactions by SDS–4 to 20% gradient gel electrophoresis and subsequent autoradiography. Lane 1, molecular weight markers; lane 2, negative control (no DNA added to the otherwise complete reaction mixture); lane 3, proteins synthesized from positive control plasmid pBestluc; lane 4, proteins synthesized from pUC9; lane 5, proteins synthesized from pT5; lane 6, proteins synthesized from pT111.

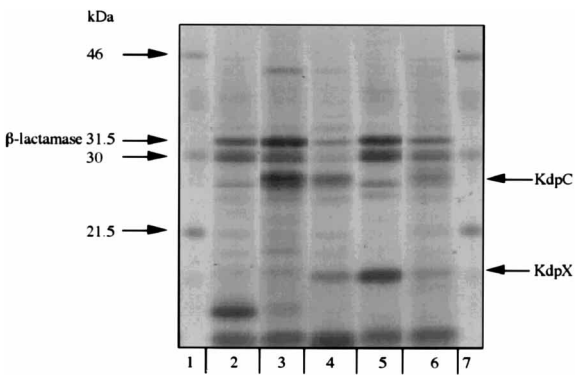

FIG. 5. Protein analysis of in vitro transcription-translation reactions in an SDS–12 to 20% gradient gel, with subsequent autoradiography. Lanes 1 and 7, molecular weight markers; lane 2, proteins synthesized from pUC9; lane 3, proteins synthesized from pTC; lane 4, proteins synthesized from pTCX; lane 5, proteins synthesized from pTX; lane 6, proteins synthesized from pT1.

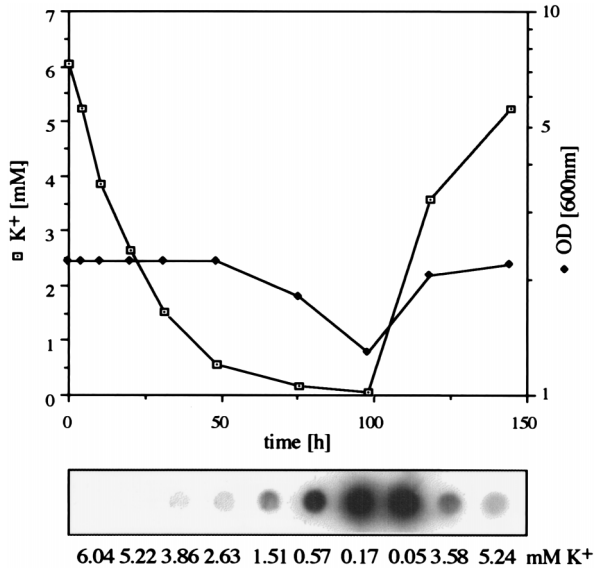

FIG. 6. Influence of decreasing the potassium concentration on growth in a continuous culture of *C. acetobutylicum*. Below, dot blot hybridization signals of RNA samples with a *kdpA* probe are presented. Potassium concentrations of the supernatants of the respective samples are indicated below the autoradiography signals.

sequence). In both cases, the same dependence of hybridization signals on the potassium concentration could be observed as in the dot blots, but it was not possible to determine the length of the mRNA transcript (data not shown). There were no distinct bands on the blots, but there was a large smear, especially at K^+ concentrations of 570 and 50 μM. This was not due to the quality of the RNA preparation since the blots were washed and hybridized again with a gene probe of a constitutive gene (*ptb*, encoding phosphotransbutyrylase) of *C. acetobutylicum*. A distinct band of the expected size became visible in each lane of the blots (data not shown). The failure to determine the length of the *kdp* mRNAs by Northern blot hybridizations led to the usage of the more sensitive RT-PCR method.

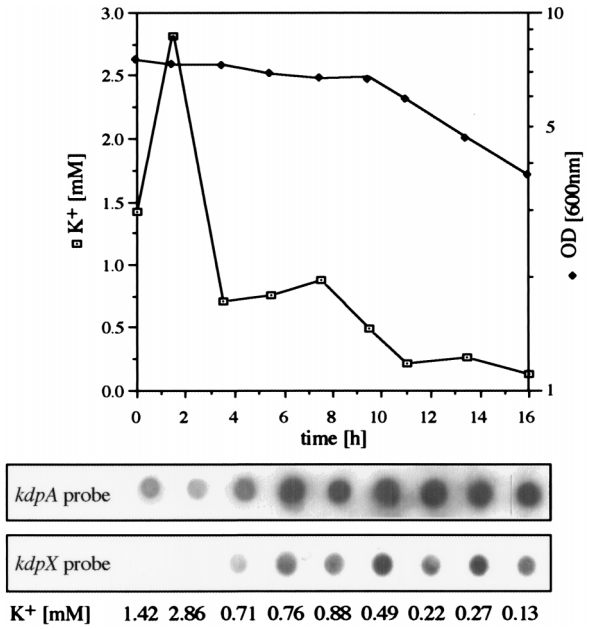

FIG. 7. Influence of decreasing the potassium concentration on growth in a continuous culture of *C. acetobutylicum*. Below, dot blot hybridization signals of RNA samples with *kdpA* and *kdpX* probes are presented. Potassium concentrations of the supernatants of the respective samples are indicated below the autoradiography signals.

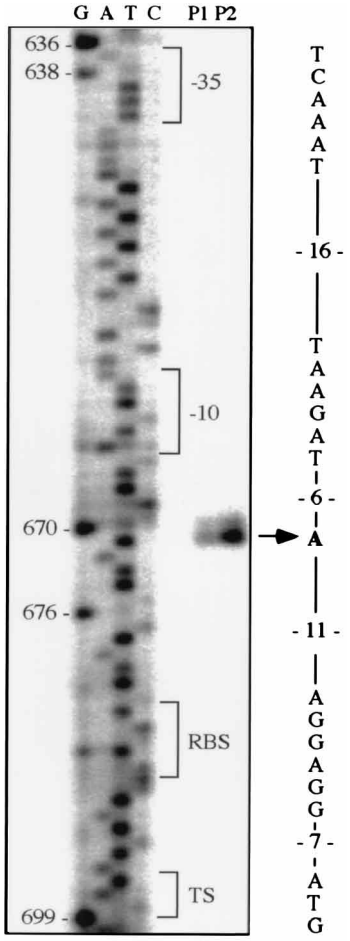

FIG. 8. Identification of the 5′ end of the *C. acetobutylicum kdpA* transcript by primer extension. The primer extension products (P1 and P2) were run on a 6% polyacrylamide gel together with a sequencing reaction with the same primer ($orfZ_p$). The sequence depicted at the right side indicates the proposed −10 and −35 promoter region, the ribosome-binding site, and the translation start; the arrow marks the transcription start point. Numbers on the left indicate the positions of the corresponding G nucleotide in the *kdp* sequence.

Oligonucleotide $kdpD_7$ was hybridized to RNA of *C. acetobutylicum* cells grown in CBM medium (no detectable *kdpA* mRNA transcripts, thus designated uninduced RNA) and with RNA of the first limitation experiment (sample 7, detectable *kdpA* transcripts in cells growing at 170 μM K^+, thus designated induced RNA). The cDNAs produced (designated accordingly as uninduced and induced cDNA) were used as templates in three different PCR assays (Fig. 9). The oligonucleotides pairs $kdpD_6$-*kdp*9.11 and $kdpD_6$-*kdp*9.10 revealed the expected fragments of 541 and 757 bp with both cDNAs. On the other hand, using the oligonucleotide pair $kdpD_6$-*kdp*9.9, we could amplify only the expected 997-bp fragment with the induced cDNA as a template (Fig. 9). PCR with the uninduced cDNA revealed no visible fragment. Oligonucleotide *kdp*9.9 hybridized to a region upstream of the *kdpD*

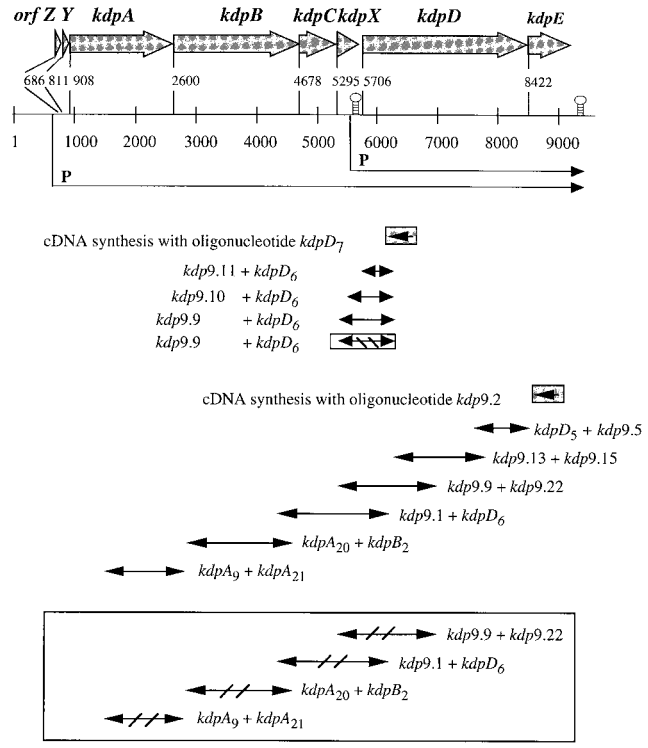

FIG. 9. Schematic ORF map of the complete chromosomal *kdp* DNA region of *C. acetobutylicum*, including the results of the RT-PCR. Stem-loop structures are indicated by hairpin symbols. The promoter regions upstream of *kdpD* and *kdpA* are marked by P's; arrows indicate positions and lengths of DNA fragments that could be amplified by PCR with the indicated oligonucleotide pairs; boxed and dashed lines represent regions that could not be amplified. The small grey boxes represents the oligonucleotides which were used for cDNA synthesis.

promoter (52), indicating that the uninduced RNA contained only mRNA transcripts starting at the *kdpD* promoter. With both RNA samples, two other cDNAs were produced with oligonucleotide *kdp*9.2, which hybridized to the 3′ end of the *kdpE* gene. Six different PCRs were performed with the produced cDNAs. PCR with the oligonucleotide pairs $kdpD_5$-*kdp*9.5 and *kdp*9.13-*kdp*9.15 revealed the expected fragments of 974 and 1,710 bp. DNA amplifications with the oligonucleotide pairs *kdp*9.9-*kdp*9.22, $kdpD_6$-*kdp*9.1, $kdpA_{20}$-$kdpB_2$, and $kdpA_9$-$kdpA_{21}$ proved to be possible only with the induced cDNA, indicating that under induced conditions, transcription of the clostridial *kdp* genes did not stop at the putative terminator structure downstream of *kdpX* but continued with the transcription of the genes *kdpD* and *kdpE*. The uninduced RNA contained only mRNA transcripts of the *kdpD* and *kdpE* genes (initiated at the promoter upstream of *kdpD*), since all attempts to amplify DNA encoding the upstream *kdp* genes failed (Fig. 9). Although the results of the RT-PCR experiments showed clearly that a common *kdpZYABCXDE* transcript was synthesized under inducing conditions, it could not be excluded that some transcripts starting upstream of *kdpA* were terminated downstream of *kdpX*. To quantify the amounts of *kdpDE* transcripts and of *kdpZYABCXDE* or *kdp ZYABCX* transcripts, we analyzed the above-described Northern blots, hybridized with a *kdpA* probe and a *kdpDE* probe. The two probes were almost equal in length and were used in the same concentration on the two identically prepared Northern blots. In both cases, the strongest hybridization signals were found with RNA sample 8 of the first limitation experiment (Fig. 6). With the thus obtained density values of the different lanes, a background subtraction including unspecific rRNA background was done. The new values (D [density] − B [background]) were finally corrected by division with the scanned area value ($D - B$/pixel^2). Since the value of the strongest *kdpDE* hybridization signal with sample 8 was still higher than that of the *kdpA* hybridization signal with sample 8 ($D - B$/pixel^2 = 119.10 with the *kdpDE* probe and 88.50 with the *kdpA* probe), both values were set as 100%, and the corresponding values of the other samples were accordingly calculated. The data are shown in Fig. 10.

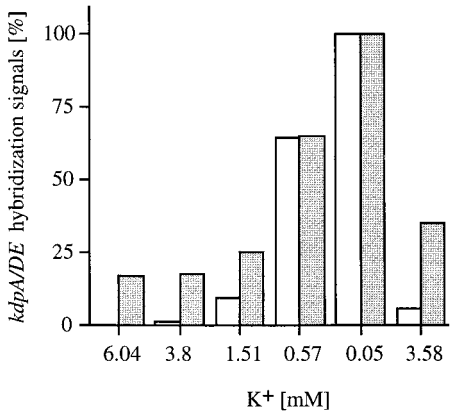

FIG. 10. Quantification of Northern blot hybridizations performed with a *kdpA* probe (white bars) and a *kdpDE* probe (grey bars) and different RNA samples from the first limitation experiment. The potassium concentrations of the supernatants of the respective samples are indicated below the bars.

In a second quantification experiment, three different oligonucleotides were used for dot blot hybridizations with three identically prepared membrane strips with 10 μg of plasmid DNA (pT5 [Fig. 1]) as a hybridization control and two different RNA samples (first limitation, sample 7) and an RNA sample, prepared from a batch culture of *C. acetobutylicum* inoculated five times in K0 medium. The oligonucleotides were chosen to quantify the region upstream (primer $kdpD_2$) and downstream (primer $kdpD_3$) of the putative terminator in comparison with a region in *kdpC* (primer $kdpC_{12}$). Data were obtained in terms of phosphostimulated luminescence and corrected as described above. With both RNA samples, we found weaker hybridization signals in the region upstream of the stem-loop structure than in the downstream region (Fig. 11).

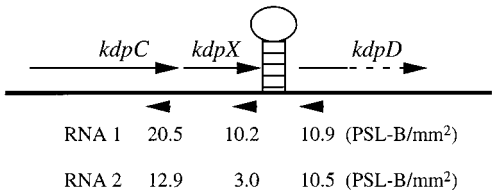

FIG. 11. Schematic representation of the *kdpCXD* region (arrows indicate the genes) with the stem-loop between *kdpX* and *kdpD*. The small leftward-directed arrows represent the oligonucleotides $kdpC_{12}$, $kdpD_2$, and $kdpD_3$. The numbers represent the quantification results revealed by hybridization of these oligonucleotides with RNA 1 (first limitation, sample 7) and RNA 2 (K^+-limited batch culture). PSL, phosphostimulated luminescence.

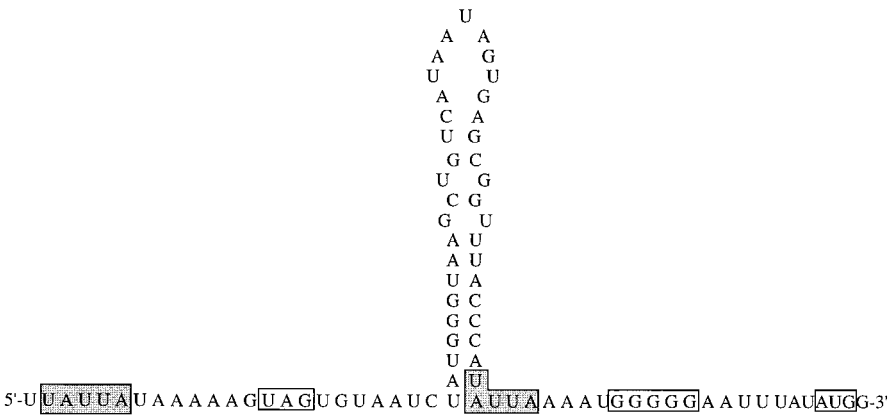

FIG. 12. Nucleotide sequence between the end of *kdpX* and the beginning of *kdpD*. The grey boxes indicate the putative recognition sites of RNase E. The white boxes represent the UAG stop codon of *kdpX*, the ribosome-binding site upstream of *kdpD*, and the AUG start codon of *kdpD*. For the stem-loop, a free energy of −18 kJ/mol (26) was calculated.

DISCUSSION

Recently, two regulatory genes of *C. acetobutylicum* have been cloned and sequenced, representing the first report on a sensor histidine kinase/response regulator system in this organism (52). Significant homology to the respective *E. coli* genes led to their identification as *kdpD* and *kdpE*. In this study, the remainder of the *kdp* system of *C. acetobutylicum* has been cloned and sequenced. Upstream of *kdpX*, a gene that has no counterpart in *E. coli*, *M. tuberculosis*, and *Synechocystis* sp. strain PCC 6803 and precedes *kdpDE*, homologous genes to *kdpA*, *kdpB*, and *kdpC* could be found. Upstream of *kdpA* are two small ORFs which might be part of the *kdp* system of *C. acetobutylicum* in that their deduced products resemble the KdpF peptide of *E. coli* (2) in size and hydropathy. Thus, *C. acetobutylicum* possesses a *kdp* DNA region very similar to that of *E. coli*. With the exception of the two small ORFs (*orfZ* and *orfY*) instead of *kdpF* and an additional ORF (*kdpX*) between *kdpC* and *kdpD*, all *kdp* genes are conserved and organized accordingly. The clostridial KdpA comprises very hydrophobic regions and a conserved region which in *E. coli* is described as a putative periplasmic K^+-binding site, suggesting a role as a integral membrane K^+-transporting protein.

KdpB of *C. acetobutylicum* showed the typical features of P-type ATPases; the most conserved motifs of this family could be found in the clostridial amino acid sequence. The description for P_3 ATPases (32) fits the clostridial KdpB in that KdpB probably is part of a protein complex consisting of KdpA, KdpB, KdpC, and possibly KdpX and does not function as a single unit like most other P-type ATPases (43). The clostridial KdpB thus represents only the second member of the P_3 group, the enterobacterial protein being so far the only known representative. Kdp from *M. tuberculosis* and *Synechocystis* sp. strain PCC 6803, identified only by sequence similarity from genome sequencing projects, might be further candidates. On one hand, KdpB resembles the non-heavy-metal-transporting P_2 ATPases because of a single pair of transmembrane fragments before the well conserved TGES sequence (24, 43, 44), which is thought to participate in vanadate and P_i binding (44) and is proposed to be responsible for phosphatase activity (44). On the other hand, the KdpB of *E. coli* is similar to the heavy-metal-transporting P_1 ATPases because of the shorter C-terminal region (32). All these features are conserved in the clostridial KdpB.

The clostridial KdpC showed no high similarity to other proteins except for KdpC of *E. coli*, *M. tuberculosis*, and *Synechocystis* sp. strain PCC 6803, and so its physiological function remains unclear. The putative membrane-spanning segment of the KdpC proteins near the N terminus is similar to the structure of the glycosylated β subunits of the a/β-heterodimeric, cation-exchange ATPase subfamily (16) which includes the ubiquitous Na^+/K^+-ATPases and the gastric H^+/K^+-ATPases. For the β subunits, an involvement in K^+-dependent reactions of the enzymes such as K^+ occlusion is suggested, and the extracellular domain might play an important role in determining the kinetics of K^+ interaction (16). The deglycosylated core proteins of the glycosylated β subunits usually have molecular masses of ca. 34 kDa, whereas the M_r of the four KdpC proteins is in the range of 22,000.

The results of the different hybridization experiments together with the results of the in vitro transcription-translation experiments revealed that *kdpX* is indeed transcribed and translated. The similarity of the hydrophobicity plots of KdpC and KdpX of *C. acetobutylicum* and KdpC of *E. coli* make it tempting to speculate that in *C. acetobutylicum*, a heterodimer of KdpC and KdpX is formed in the active complex, whereas in *E. coli*, a homodimer of KdpC serves this function. This speculation might be supported by a possible function of the small hydrophobic peptides as a "glue," of which two (OrfZ and OrfY) have been found in *C. acetobutylicum*, whereas only one (KdpF) is present in *E. coli*.

Induction of the genes is clearly potassium dependent. Transcription occurred from two different promoters. In media of high potassium concentration, only the genes *kdpD* and *kdpE* are transcribed from the *kdpD* promoter (52). This transcription ensures a constitutive but very low expression of the *kdpDE* operon (52). As soon as the potassium concentration decreased and became a growth-limiting factor, transcription of the *kdp* genes started upstream of *orfZ*, and all *kdp* genes, including *kdpD* and *kdpE*, which encode for the *kdp* sensor histidine kinase/response regulator system, were transcribed together, as indicated by the results of the RT-PCR. Induction by lowering the potassium concentration obviously prevented transcription from the *kdpD* promoter, since under these conditions determination of the respective mRNA start point failed. This also explains why Northern hybridization with a *kdpDE* probe revealed the same dependence on the potassium concentration as experiments using a *kdpA* probe. In *E. coli*, similar experiments have not been performed. A promoter has

been identified upstream of *kdpD*, in the *kdpC* gene (40). Transcriptional fusions of *lacZ* to *kdp* genes indicated increased expression, attributed to read-through from transcription of *kdpFABC* (2). However, the authors assumed that about 90% of all transcripts, regardless of where they begin, terminate early in *kdpD* (40). In contrast, experiments aiming at quantitation of KdpD by antibodies clearly showed that the amount of KdpD was increased under potassium-limiting conditions (54). Thus, the situation in *E. coli* might be the same as in *C. acetobutylicum*, where the *kdp* genes are transcribed together with *kdpD* and *kdpE*. At first glance, it does not make sense that transcription of the regulator genes, whose products control expression of the Kdp system, is also increased by low potassium concentrations. However, it could be that KdpD and KdpE not only activate transcription of the *kdp* system but together serve as a master unit playing a pivotal role in general osmoregulation. Future experiments will try to solve this question.

Northern hybridizations revealed that the *kdp* mRNAs are very unstable, whereas other mRNA transcripts were identified on the same blots without problems. The fast degradation of *kdp* mRNA seems to be part of the complex regulation of this system. The common *kdpZYABCXDE* transcript is detectable only with RT-PCR; on a Northern blot, many degradation products in a range of 8,000 to 1,000 ribonucleotides become visible. The results of the different hybridization experiments indicate that the region upstream of the stem-loop structure between *kdpX* and *kdpD* is much more unstable than the regions within the *kdpA*, *kdpC*, and *kdpD* genes. In recent years, much progress has been made in identification of enzymes which are involved in mRNA degradation, and it seems generally accepted that mRNA turnover plays a central role in determining levels of protein synthesis (4, 9, 21). Many reports describe specific sequences, and structural features of an mRNA probably determine its stability (for examples, see references 5, 12, 15, 17, 37, 55, and 60). A recent review (18) summarizes features of RNase E, which is known to play a general role in mRNA decay. Naureckiene and Uhlin (37) describe RNase E as a single-strand-specific endoribonuclease and a high A/U content as a common feature of the cleaved sequences. A pentanucleotide consensus sequence (G/A)′A′UU(A/U) followed by a stable secondary structure has been proposed as the cleavage site of RNase E (21). Recent data have shown that RNase E can cleave oligoribonucleotides lacking a stem-loop structure (36), but it also has been suggested that stem-loops in the vicinity of the RNase E cleavage site could stabilize mRNA structure and maintain the single-strandedness of the cleavage site (19, 33). It has also been shown that destabilization of such a stem-loop structure reveals probably cryptic RNase E cleavage sites, suggesting a shielding role of these structures in RNase E recognition (37). Taking into account all of these recent findings, it is possible to propose an RNase E cleavage site in the clostridial nucleotide sequence between the end of *kdpX* and the beginning of *kdpD* (Fig. 12). In accordance with the consensus sequence prepared by Ehretsmann et al. (21), we found two possible cleavage sites, one single stranded and the other partially folded in the stem-loop. A cleavage of the mRNA transcript at the single-stranded site would explain the weaker hybridization signals of the *kdpX* probes in comparison to those of *kdpA* and *kdpD*. The downstream cleavage product would be more stable than the upstream mRNA because of the stem-loop structure, whereas the free 3′ end of the *kdpZYABCX* transcript could be degraded by the action of 3′-to-5′ exonucleases. A cleavage of the mRNA at this position could also be possible in the *kdpDE* transcript, which is formed under uninducing conditions, since none of the translation signals would be deleted by this cleavage (Fig. 12). Nevertheless, this RNase E cleavage model is only a speculation since we know nothing about RNA-degrading enzymes in *C. acetobutylicum.*

For the DNA region upstream of *kdpA* in *E. coli*, a KdpE-binding sequence, a 21-bp target site of the *trans*-acting activator protein KdpE, has been described as an essential sequence for activation of the *kdpA* promoter. Five stretches of T's occur periodically around this bending center (51). The distance between the −35 region of the *kdpA* promoter and the KdpE-binding sequence is 9 bp. The KdpE-binding sequence was shown to be 5′-TTTATACTTTTTTTACACCCC-3′. Upstream of the clostridial *orfZY*/*kdpA* promoter, a similar region with the sequence 5′-TTTATACTTTCTTAACACCTG-3′ and a distance of 16 bp to the −35 box was identified. However, stretches of T's are common in DNA of *C. acetobutylicum*, since this organism has a G+C content of 28 to 29 mol% (6). Thus, it remains to be determined whether this region represents a KdpE-binding site.

ACKNOWLEDGMENTS

We are grateful to K. Altendorf, W. Epstein, and W. Puppe for continuous advice and critical and stimulating discussions.

This work was supported by a grant from the Deutsche Forschungsgemeinschaft.

REFERENCES

1. **Abee, T., A. Siebers, K. Altendorf, and W. N. Konings.** 1992. Isolation and characterization of the high-affinity K^+-translocating ATPase from *Rhodobacter sphaeroides*. J. Bacteriol. **174:**6911–6917.
2. **Altendorf, K., and W. Epstein.** 1993. Kdp-ATPase of *Escherichia coli*. Cell. Physiol. Biochem. **4:**160–168.
3. **Altschul, S. F., W. Gish, W. Miller, E. W. Myers, and D. J. Lipman.** 1990. Basic local alignment search tool. J. Mol. Biol. **215:**403–410.
4. **Apirion, D.** 1973. Degradation of RNA in *Escherichia coli*. A hypothesis. Mol. Gen. Genet. **122:**313–322.
5. **Arraiano, C. M., S. D. Yancey, and S. R. Kushner.** 1993. Identification of endonucleolytic cleavage sites involved in decay of *Escherichia coli trxA* mRNA. J. Bacteriol. **175:**1043–1052.
6. **Bahl, H., and P. Dürre.** 1993. Clostridia, p. 285–323. *In* H.-J. Rehm and G. Reed (ed.), Biotechnology, 2nd ed. vol. 1. VCH Verlagsgesellschaft mbH, Weinheim, Germany.
7. **Bakker, E. P.** 1992. Cell K^+ and K^+ transport systems in prokaryotes, p. 205–224. *In* E. P. Bakker (ed.), Alkali cation transport systems in prokaryotes. CRC Press, Boca Raton, Fla.
8. **Bakker, E. P.** 1992. Low-affinity K^+ uptake systems, p. 253–276. *In* E. P. Bakker (ed.), Alkali cation transport systems in prokaryotes. CRC Press, Boca Raton, Fla.
9. **Belasco, J. G., and C. F. Higgins.** 1988. Mechanism of mRNA decay in bacteria: a perspective. Gene **72:**15–23.
10. **Bertram, J., and P. Dürre.** 1989. Conjugal transfer and expression of streptococcal transposons in *Clostridium acetobutylicum*. Arch. Microbiol. **151:** 551–557.
11. **Booth, I. R., and C. F. Higgins.** 1990. Enteric bacteria and osmotic stress: intracellular potassium glutamate as a secondary signal of osmotic stress? FEMS Microbiol. Rev. **75:**239–246.
12. **Bouvet, P., and J. G. Belasco.** 1992. Control of RNase E-mediated RNA degradation by 5′-terminal base pairing in *E. coli*. Nature **360:**488–491.
13. **Buluwela, L., A. Forster, T. Boehm, and T. H. Rabbitts.** 1989. A rapid procedure for colony screening using nylon filters. Nucleic Acids Res. **17:**452.
14. **Buurman, E. T., K.-T. Kim, and W. Epstein.** 1995. Genetic evidence for two sequentially occupied K^+ binding sites in the Kdp transport ATPase. J. Biol. Chem. **270:**6678–6685.
15. **Cam, K., G. Rome, H. M. Krisch, and J. P. Bouche.** 1996. RNase E processing of essential cell division genes mRNA in *Escherichia coli*. Nucleic Acids Res. **24:**3065–3070.
16. **Chow, D. C., and J. G. Forte.** 1995. Functional significance of the β-subunit for heterodimeric P-type ATPases. J. Exp. Biol. **198:**1–17.
17. **Chow, J., and P. P. Dennis.** 1994. Coupling between mRNA synthesis and mRNA stability in *Escherichia coli*. Mol. Microbiol. **11:**919–931.
18. **Cohen, S. N., and K. J. McDowall.** 1997. RNase E: still a wonderfully mysterious enzyme. Mol. Microbiol. **23:**1099–1106.
19. **Cormack, R. S., and G. A. Mackie.** 1992. Structural requirements for the processing of *Escherichia coli* 5S ribosomal RNA by RNase E *in vitro*. J. Mol. Biol. **228:**1078–1090.

20. **Devereux, J., P. Haeberli, and O. Smithies.** 1984. A comprehensive set of sequence analysis programs for the VAX. Nucleic Acids Res. **12:**387–395.
21. **Ehretsmann, C. P., A. J. Garpousis, and H. M. Krisch.** 1992. mRNA degradation in procaryotes. FASEB J. **6:**3186–3192.
22. **Epstein, W.** 1985. The Kdp system, a bacterial transport ATPase. Curr. Top. Membr. Transp. **23:**153–175.
23. **Epstein, W.** 1986. Osmoregulation by potassium transport in *Escherichia coli*. FEMS Microbiol. Rev. **39:**73–78.
24. **Fagan, M. J., and M. H. Saier, Jr.** 1994. P-type ATPases of eukaryotes and bacteria: sequence analyses and construction of phylogenetic trees. J. Mol. Evol. **38:**57–99.
25. **Fischer, R. J., J. Helms, and P. Dürre.** 1993. Cloning, sequencing, and molecular analysis of the *sol* operon of *Clostridium acetobutylicum*, a chromosomal locus involved in solventogenesis. J. Bacteriol. **175:**6959–6969.
26. **Freier, S. M., R. Kierzek, J. A. Jaeger, N. Sugimoto, M. H. Caruthers, T. Neilson, and D. H. Turner.** 1986. Improved free-energy parameters for prediction of RNA duplex stability. Proc. Natl. Acad. Sci. USA **83:**9373–9377.
27. **Gerischer, U., and P. Dürre.** 1990. Cloning, sequencing, and molecular analysis of the acetoacetate decarboxylase gene region from *Clostridium acetobutylicum*. J. Bacteriol. **172:**6907–6918.
28. **Gerischer, U., and P. Dürre.** 1992. mRNA analysis of the *adc* gene region of *Clostridium acetobutylicum* during the shift to solventogenesis. J. Bacteriol. **174:**426–433.
29. **Hafer, J., A. Siebers, and E. P. Bakker.** 1989. The high-affinity K^+-translocating ATPase complex from *Bacillus acidocaldarius* consists of three subunits. Mol. Microbiol. **3:**487–495.
30. **Kaneko, T., S. Sato, H. Kotani, A. Tanaka, E. Asamizu, Y. Nakamura, N. Miyajima, M. Hirosawa, M. Sugiura, S. Sasamoto, T. Kimura, T. Hosouchi, A. Matsuno, A. Muraki, N. Nakazaki, K. Naruo, S. Okumara, S. Shimpo, C. Takeuchi, T. Wada, A. Watanabe, M. Yamada, M. Yasuda, and S. Tabata.** 1996. Sequence analysis of the genome of the unicellular cyanobacterium *Synechocystis sp.* strain PCC6803. II. Sequence determination of the entire genome and assignment of potential protein-coding regions. DNA Res. **3:**109–136.
31. **Kyte, J., and R. F. Doolittle.** 1982. A simple method for displaying the hydropathic character of a protein. J. Mol. Biol. **157:**105–132.
32. **Lutsenko, S., and J. H. Kaplan.** 1995. Organization of P-type ATPases: significance of structural diversity. Biochemistry **34:**15607–15613.
33. **Mackie, G. A., and J. L. Genereaux.** 1993. The role of RNA structure in determining RNase E-dependent cleavage sites in the mRNA for ribosomal protein S20 *in vitro*. J. Mol. Biol. **234:**998–1012.
34. **Marck, C.** 1988. 'DNA Strider': a 'C' program for the fast analysis of DNA and protein sequences on the Apple Macintosh family of computers. Nucleic Acids Res. **16:**1829–1836.
35. **Marmur, J.** 1961. A procedure for the isolation of deoxyribonucleic acid from microorganisms. J. Mol. Biol. **3:**208–218.
36. **McDowall, K. J., V. R. Kaberdin, S. W. Wu, S. N. Cohen, and S. Lin-Chao.** 1995. Site specific RNase E cleavage of oligonucleotides and inhibition by stem-loops. Nature **374:**287–290.
37. **Naureckiene, S., and B. E. Uhlin.** 1996. *In vitro* analysis of mRNA processing by RNase E in the *pap* operon of *Escherichia coli*. Mol. Microbiol. **21:**55–68.
38. **O'Brien, R. W., and J. G. Morris.** 1971. Oxygen and the growth and metabolism of *Clostridium acetobutylicum*. J. Gen. Microbiol. **68:**307–318.
39. **Oelmüller, U., N. Krüger, A. Steinbüchel, and C. G. Friedrich.** 1990. Isolation of prokaryotic RNA and detection of specific mRNA with biotinylated probes. J. Microbiol. Methods **11:**73–84.
40. **Polarek, J. W., G. Williams, and W. Epstein.** 1992. The products of the *kdpDE* operon are required for expression of the Kdp ATPase of *Escherichia coli*. J. Bacteriol. **174:**2145–2151.
41. **Sambrook, J., E. F. Fritsch, and T. Maniatis.** 1989. Molecular cloning: a laboratory manual, 2nd ed. Cold Spring Harbor Laboratory, Cold Spring Harbor, N.Y.
42. **Sauer, U., A. Treuner, M. Buchholz, J. D. Santangelo, and P. Dürre.** 1994. Sporulation and primary sigma factor homologous genes in *Clostridium acetobutylicum*. J. Bacteriol. **176:**6572–6582.
43. **Serrano, R.** 1988. Structure and function of proton translocating ATPase in plasma membranes of plants and fungi. Biochim. Biophys. Acta **947:**1–28.
44. **Serrano, R.** 1989. Structure and function of plasma membrane ATPase. Annu. Rev. Plant Physiol. Plant Mol. Biol. **40:**61–94.
45. **Siebers, A., and K. Altendorf.** 1988. The K^+-translocating Kdp-ATPase from *Escherichia coli*: purification, enzymatic properties and production of complex- and subunit-specific antisera. Eur. J. Biochem. **178:**131–140.
46. **Siebers, A., and K. Altendorf.** 1992. K^+-translocating Kdp-ATPases and other bacterial P-type ATPases, p. 205–224. *In* E. P. Bakker (ed.), Alkali cation transport systems in prokaryotes. CRC Press, Boca Raton, Fla.
47. **Simoneau, P., and J. Labarère.** 1991. Evidence for the presence of two distinct membrane ATPases in *Spiroplasma citri*. J. Gen. Microbiol. **137:**179–186.
48. **Snavely, M. D., C. G. Miller, and M. E. Maguire.** 1991. The *mgtB* Mg^{2+} transport locus of *Salmonella typhimurium* encodes a P-type ATPase. J. Biol. Chem. **266:**815–823.
49. **Stumpe, S., A. Schlösser, M. Schleyer, and E. P. Bakker.** 1996. K^+ circulation across the prokaryotic cell membrane: K^+-uptake systems, p. 473–499. *In* W. N. Konings, H. R. Kaback, and J. S. Lolkema (ed.), Transport processes in eukaryotic and prokaryotic organisms. Handbook of biological physics, vol. II. Elsevier Science, Amsterdam, The Netherlands.
50. **Suggs, S. V., T. Hirose, T. Miyake, E. H. Kawashima, M. J. Johnson, K. Itakura, and R. B. Wallace.** 1981. Use of synthetic oligodeoxyribonucleotides for the isolation of specific cloned DNA sequences, p. 683–693. *In* D. D. Brown and C. F. Fox (ed.), Developmental biology using purified genes. Academic Press, New York, N.Y.
51. **Sugiura, A., K. Nakashima, and T. Mizuno.** 1993. Sequence-directed DNA curvature in activator-binding sequence in the *Escherichia coli kdpABC* promoter. Biosci. Biotechnol. Biochem. **57:**356–357.
52. **Treuner-Lange, A., and P. Dürre.** 1996. Genetic analysis of *kdpD*/*E*, a sensor histidine kinase/response regulator system in *Clostridium acetobutylicum*. Anaerobe **2:**351–363.
53. **Vieira, J., and J. Messing.** 1982. The pUC plasmids, an M13mp7-derived system for insertion mutagenesis and sequencing with universal primers. Gene **19:**259–268.
54. **Voelkner, P., W. Puppe, and K. Altendorf.** 1993. Characterization of the KdpD protein, the sensor kinase of the K^+-translocating Kdp system of *Escherichia coli*. Eur. J. Biochem. **217:**1019–1026.
55. **von Gabain, A., J. G. Belasco, J. L. Schottel, A. C. Chang, and S. N. Cohen.** 1983. Decay of mRNA in *Escherichia coli*: investigation of the fate of specific segments of transcripts. Proc. Natl. Acad. Sci. USA **80:**653–657.
56. **Walderhaug, M. O., E. D. Litwick, and W. Epstein.** 1989. Wide distribution of homologs of *Escherichia coli* Kdp K^+-ATPases among Gram-negative bacteria. J. Bacteriol. **171:**1192–1195.
57. **Walderhaug, M. O., J. W. Polarek, P. Voelkner, J. M. Daniel, J. E. Hesse, K. Altendorf, and W. Epstein.** 1992. KdpD and KdpE, proteins that control expression of the *kdpABC* operon, are members of the two-component sensor-effector class of regulators. J. Bacteriol. **174:**2152–2159.
58. **Yanisch-Perron, C., J. Vieira, and J. Messing.** 1985. Improved M13 phage cloning vectors and host strains: nucleotide sequence of the M13mp18 and pUC19 vectors. Gene **33:**103–119.
59. **Young, M., N. P. Minton, and W. L. Staudenbauer.** 1989. Recent advances in the genetics of the clostridia. FEMS Microbiol. Rev. **63:**301–326.
60. **Zilhão, R., F. Cairrão, P. Régnier, and C. M. Arraiano.** 1996. PNPase modulates RNase II expression in *Escherichia coli*: implications for mRNA decay and cell metabolism. Mol. Microbiol. **20:**1033–1042.